Published in final edited form as:
Bioresour Technol. 2011 March ; 102(6): 4518–4523. doi:10.1016/j.biortech.2010.12.087.

Reversible swelling of the cell wall of poplar biomass by ionic liquid at room temperature

Marcel Lucas[a], **Greg L. Wagner**[a], **Yoshiharu Nishiyama**[b], **Leif Hanson**[c], **Indira P. Samayam**[c], **Constance A. Schall**[c], **Paul Langan**[d], and **Kirk D. Rector**[a,*]

[a]Chemistry Division, Los Alamos National Laboratory, Los Alamos, NM 87545, USA

[b]Centre de Recherches sur les Macromolécules Végétales – CNRS, affiliated with the Joseph Fourier University of Grenoble, BP 53, 38041 Grenoble Cedex 9, France

[c]Department of Chemical Engineering, University of Toledo, 2801 W. Bancroft, Toledo, OH 43606, USA

[d]Bioscience Division, Los Alamos National Laboratory, Los Alamos, NM 87545, USA

Abstract

Time-resolved autofluorescence, Raman microspectroscopy, and scanning microprobe X-ray diffraction were combined in order to characterize lignocellulosic biomass from poplar trees and how it changes during treatment with the ionic liquid 1-*n*-ethyl-3-methylimidazolium acetate (EMIMAC) at room temperature. The EMIMAC penetrates the cell wall from the lumen, swelling the cell wall by about a factor of two towards the empty lumen. However, the middle lamella remains unchanged, preventing the cell wall from swelling outwards. During this swelling, most of the cellulose microfibrils are solubi-lized but chain migration is restricted and a small percentage of microfibrils persist. When the EMIMAC is expelled, the cellulose recrystallizes as microfibrils of cellulose I. There is little change in the relative chemical composition of the cell wall after treatment. The action of EMIMAC on the poplar cell wall at room temperature would therefore appear to be a reversible swelling and a reversible decrystallization of the cell wall.

Keywords

Pretreatment; Lignocellulosic biomass; Cellulose; Wood; Ionic liquid

1. Introduction

Lignocellulosic biomass, the fibrous material derived from plant cell walls, is a potential clean and renewable, non-food feedstock for liquid fuel and chemical production in future biorefineries (Alvira et al., 2010). The conversion of lignocellulosic biomass, comprised primarily of lignin, hemicellulose and cellulose, into simple sugars constitutes a core barrier for producing products from the sugar platform (Chen et al., 2007). Current pretreatments of biomass that improve the efficiency of its conversion are energy-intensive and generate inhibitory products (Alvira et al., 2010; Yang and Wyman, 2008). Recently, Ionic Liquids (ILs) have been investigated by several groups as a promising approach for pre-treatment (Alvira et al., 2010). ILs not only disrupt the plant cell wall and separate its cellulosic, hemicellulosic, and lignin components, but also disrupt the crystallinity of cellulose making

*Corresponding author. Address: Los Alamos National Laboratory, P.O. Box 1663, MS J567, Los Alamos, NM 87545, USA. Tel.: +1 505 667 9457; fax: +1 505 667 0440. kdr@lanl.gov (K.D. Rector).

it more efficiently hydrolyzed into sugars by enzymes (Dadi et al., 2006, 2007; Samayam and Schall, 2010; Sun et al., 2009). Some advantages of this approach are that it is non-derivatizing, that it does not produce fermentation inhibitors, and that it is amenable for "easy recovery" of the ILs employed in the pretreatment. Several studies showed that total dissolution and separation of the cellulosic, hemicellulosic, and lignin components of biomass can be achieved at elevated temperatures (Fort et al., 2007). The optimum temperature and time for completely solubilizing the cell walls of switch-grass are 160 °C and 3 h (Li et al., 2010). However, these elevated temperatures add significantly to the cost of lignocellulosic biorefining. The development of a room temperature IL pretreatment process would be of high value.

In this study, the time-dependent solubilization of lignocellulosic biomass from poplar trees by the IL 1-*n*-ethyl-3-methylimida-zolium acetate (EMIMAC) is investigated at room temperature. EMIMAC is one of several ILs that were identified as effective in enhancing biomass saccharification (Kosan et al., 2008; Lee et al., 2009; Samayam and Schall, 2010) and was selected for this study due to its ready rejection of dissolved cellulose by the addition of an anti-solvent, such as water or ethanol (Zhu et al., 2006), and its lower toxicity (Romero et al., 2008). Because of the compositional and structural complexity of the cell wall and its interaction with ILs, no one experimental technique can provide a detailed understanding of the chemical composition and structure of lignocellulosic biomass and the time dependent impact of pretreatment. Therefore, the approach of combining several non-invasive experimental techniques was taken to characterize the intact plant cell wall at multiple length scales. Time-resolved scanning microprobe X-ray diffraction (SMXD) methods can provide information on the ordered regions in cellulose fibers over the Å to nm level of detail (Igarashi et al., 2007; Nishiyama et al., 2010; Wada et al., 2004) and was used to determine how the size, crystal structure, and crystallinity of cellulose fibers change as a function of time under the action of EMIMAC at room temperature. To address changes over longer length scales, time-resolved autofluorescence was used to map the different cell wall components (Singh et al., 2009), and monitor physical changes at the nm–μm scale. Raman microspectroscopy was included in this study to monitor changes in chemical composition (Gierlinger and Schwanninger, 2006) in the secondary cell wall at different stages of treatment with EMIMAC.

2. Methods

2.1. Sample preparation

Poplar (*Populus tremuloides*) was selected as the source of bio-mass because it has great potential as a highly abundant, low cost, non-food feedstock for the production of biofuels. Poplar species have cellulose, hemicelluloses, and lignin contents ranging from 42% to 49%, 16% to 23%, and 21% to 29%, respectively (Sannigrahi et al., 2010). Radial and axial sections of various thicknesses were cut from a block of poplar wood using a microtome. Axial sections for autofluorescence microscopy and Raman microspectroscopy measurements were dried in an oven overnight between two glass slides at 60 °C to prevent curling. EMIMAC (>90% purity) was purchased from Sigma-Aldrich (St. Louis, Missouri). Radial sections of poplar were mounted over a frame for X-ray diffraction. Dewaxed ramie fibers were purchased from a textile dealer and bundles of aligned fibers were mounted over a frame for X-ray diffraction measurements.

2.2. Laser scanning fluorescence microscopy

A series of time-lapse autofluorescence images was collected over a period of 3 h from a 50 μm thick axially microtomed poplar section as it was treated with EMIMAC at room temperature. Images were collected with a Zeiss LSM 510 confocal system mounted on a

Zeiss Axiovert 200 M inverted microscope, with a pixel dwell time of about 5 μs. A 514 nm argon ion laser was used for excitation and the fluorescence signal was collected with the Meta detector over a 600–620 nm range with a 63× oil objective (NA 1.4). The same instrument was used to collect emission spectra from the sample. Spatial coordinates with respect to one of the sample corners from the microscope stage and brightfield images at different magnifications allowed for the capture of autofluorescence images from the same poplar cells after any sample preparation step. The resulting images were analyzed using LabVIEW in order to extract the total cell area, A_{cell}, defined as the area within the cell corners, and the empty lumen area, A_{lumen}, determined using a flooding method that identifies all the pixels below a defined intensity level. These parameters were measured in several locations in each image in order to obtain a measure of the experimental errors. The difference between A_{cell} and A_{lumen} corresponds to the area occupied by the cell wall, A_{wall}.

2.3. Raman microspectroscopy

Raman microspectra were acquired from 50 μm thick axially microtomed poplar samples using a Bruker Optics Senterra upright microscope with an Olympus MPlan 20× (NA 0.40) objective. A halogen lamp was used to illuminate the sample for brightfield visualization for sample positioning. Brightfield images and Raman spectra were collected using transfer optics in the trinocular head (Olympus U-TV1X-2) and imaged using an Infinity 1 digital color camera (Lumenera Corp., Ottawa, ON). Raman experiments were performed using a 785 nm excitation light point focused to an approximate size of 2 μm^2 using a total power of 100 mW. Various locations in randomly selected cells were used to acquire the data. Spectra were acquired in triplicate to compare results. The Raman signal was transferred through a 50 μm slit of a spectrometer and dispersed using a 1200 lines/mm grating, which is moved to acquire spectra with Raman shifts in the 100–600 cm^{-1} range. Frequency calibration of the grating positions was performed using Ne and Ar internal standards. The data were recorded using a TE-cooled CCD array detector (Andor, DU420A-OE-152). The spectral resolution of the spectrograph ranges from 3 to 5 cm^{-1} across the Raman data range acquired. The data were acquired during 10 s integration time with 5 coadditions. Processing of the data included dark background subtraction, NIST-calibrated spectral flat field correction, baseline correction using a concave rubberband correction algorithm, and normalization. Raman microspectra were acquired at room temperature from dry poplar, poplar swollen in water, poplar swollen in EMIMAC, and finally poplar swollen in EMIMAC and then washed in water. A table showing the major band positions, and chemical assignments, when known from the literature, are shown in Table S1 in Supplementary data.

2.4. Scanning microprobe X-ray diffraction

Poplar and ramie samples were mounted on the scanning stage of the BioCAT beam line at the Advanced Photon Source, in microprobe geometry, and two series of diffraction images were recorded with a CCD detector as the samples were treated with EMIMAC. The sample to detector distance was 50 mm and the FWHM of the direct beam on the detector was about 8 μm. The exposure time varied depending on the diffracting power of the sample; it was 10 s for ramie fibers, and 2 s for radial sections of poplar around 40 μm thick. The detector duty time was ~15 s (λ = 1.033 Å). Samples were kept under a stream of dry nitrogen, at room temperature, to minimize water absorption. Whilst collecting the two series of images, the samples were stepped by 10 μm in between each image, in order to reduce the effects of radiation damage. In the case of ramie, the X-ray beam was positioned at the center of an individual ramie fiber of about 70 μm in diameter and then the sample was moved along the fiber axis between images. The ramie fiber diffraction direction is approximately vertical. In both cases, after recording the first few images, a drop of anhydrous EMIMAC was applied directly to the sample, and further images were collected as the IL penetrated the sample.

EMIMAC was then forced out of the sample by humidifying the nitrogen gas stream. In the case of poplar, the time series only corresponded to 9 images, with the EMIMAC being expelled after only a few minutes. In the case of ramie, the time series lasted over an hour and at certain points during the series, when the diffraction data appeared not to be changing significantly, further drops of EMIMAC were applied to the sample.

Detector images were processed in batch mode in order to extract the radial profile widths and the relative intensities of equatorial reflections. For each detector image, first the sample tilt and rotation were determined by fitting the polar angles of 4 equivalent reflections at constant reciprocal radius. The image was then transformed into polar reciprocal space where contributions from different parts of the detector image to each pixel in polar reciprocal space were averaged with an associated standard deviation. This standard deviation allowed the scattering background to be estimated using the maximum entropy method. The radial profile widths and intensities of the principal equatorial reflections up to a resolution of 3.8 Å (corresponding to 3 composite diffraction peaks) were measured at the beginning of each series.

Two crystal allomorphs exist for the cellulose that occurs naturally in plant cell walls, cellulose I_α and I_β, which are collectively referred to as cellulose I. Cellulose I_α has space group *P1* with reduced unit cell of $a = 6.717$ Å, $b = 5.962$ Å, $c = 10.40$ Å, $\alpha = 118.08°$, $\beta = 114.80°$, and $\gamma = 80.37°$; cellulose I_β has space group $P2_1$ with a reduced unit cell of $a = 7.784$ Å, $b = 8.201$ Å, $c = 10.38$ Å, and $\gamma = 96.5°$ (Nishiyama et al., 2002, 2003). The (1 0 0), (0 1 0) and (1 1 0) reflections from I_α overlap with the (1 -1 0), (1 1 0) and (2 0 0) reflections from I_β, respectively. In the analysis, the overlapping contributions were treated as one peak, and they are referred by their I_β Miller indices. However, as the series progressed it became difficult to measure these values accurately. In the case of poplar, it was difficult to measure radial profiles immediately after the application of EMIMAC. In the case of ramie, it was most instructive to represent just the changes in overall intensities of the I_β equatorial reflections as a function of time, and to display the equatorial traces as a time series. The X-ray diffraction patterns from poplar were not background subtracted in order to illustrate the presence of diffuse scattering from EMIMAC. The X-ray diffraction patterns collected from ramie were background subtracted, using a circularly symmetric function and CCP13 software (http://www.fibre-diffraction.ac.uk/small-angle/Software/FibreFix. html).

3. Results and discussion

3.1. Autofluorescence studies

The cell wall of poplar is organized in several layers that have different compositions and structures that include the middle lamella (ML), lumen (L), ray parenchyma cells (R), cell corners (CC) and the S2 sub-layer of the secondary cell wall (see Fig. S1 in Supplementary data) (Côté et al., 1969). Before application of EMIMAC, the weak autofluorescence signal comes mainly from the reflection of the incident laser bleeding over the detection window. The relatively higher intensity in the S2 sub-layer is attributed to its higher density compared to the middle lamella. The boundary between L and S2 is sharply defined.

After the first few images, anhydrous EMIMAC was dropped onto the sample. Upon addition of EMIMAC, the cell walls swell and the overall autofluorescence intensity increases (see Fig. S2 in Supplementary data). The boundaries between S2 and L become particularly bright. Emission spectra from the poplar samples with excitations at 458, 488 and 514 nm indicate that the overall bright autofluorescence from the sample during the pretreatment is mainly from EMIMAC (data not shown). The relatively high intensity at the

boundary between S2 and L might indicate preferential adsorption of EMIMAC to that surface. As time progresses, this boundary becomes rounded as though bulging.

Normalized measurements of the total cell area A_{cell}, lumen area A_{lumen} and cell wall area A_{wall} for four different latewood cells near a ray parenchyma cell over the course of the series are shown in Fig. 1. The four different cells, referred to as A, B, C and D, were chosen to span the range of different sizes present, and had initial values of (A) 540 μm^2, (B) 350 μm^2, (C) 250 μm^2 and (D) 90 μm^2 for A_{cell} at the start of the EMIMAC treatment. The values of A_{cell} remain fairly constant. However, the values of A_{lumen} are reduced by 40–83%, depending on the size of the cell (Fig. 1b). For the smallest cells (not used for measurements), the lumen completely collapsed, i.e. A_{lumen} becomes zero. The values of A_{wall} increase by 60–100%.

This swelling results in a reduction in the size of the lumen (A_{lumen}) but the overall size of the cells (A_{cell}) remains constant, i.e. the swelling occurs inwards with the ML remaining unchanged. EMIMAC would appear to be preferentially adsorbed to the cell wall at its inner surface with the lumen. It has little effect on the ML at the outer surface of the cell wall, suggesting that EMIMAC penetrates the cell wall preferentially from the lumen, causing the cell wall to swell inwards into the lumen cavity. The unchanging ML would appear to prevent the outward swelling of the cells.

At the end of the three-hour treatment, EMIMAC was expelled from the cell walls by washing in de-ionized water. The expulsion of EMIMAC resulted in a dramatic decrease in the intensity of autofluorescence from the cell wall, although the ML remains bright. A contrast inversion was observed and was partially due to the fact that the sample is out-of-focus after the introduction of water. The boundaries between S2 and L become sharp again. There is an immediate increase in both A_{cell} by 11–25% and also A_{lumen} by 25–280%, with little further change afterwards (Fig. 1). The values of A_{lumen} increase to about 75–85% of their original sizes (Fig. 1b). Although the thickness of the S2 layer decreases on displacement of EMIMAC by water, A_{wall} remains fairly constant. This is explained by the simultaneous increase of the ML area upon water introduction.

Although EMIMAC appears to have little effect on the ML, water allows it to expand, thus allowing the cells to increase in size and the already swollen cell walls to change shape and decompress outwards, whilst occupying the same area. The lumens of the smallest cells remain completely collapsed and occupied by material that has been released from S2.

For comparison, the time-lapse experiment was repeated with de-ionized water only. After the first few images (see Figs. S3 and S4 in Supplementary data), water was dropped onto the sample and then dehydration of the sample was monitored over a period of 6 h. In this case, there was an initial increase in A_{cell} over a period of about 10 min, and then a slower decrease back to the original value as water evaporated from the sample over the course of 6 h. During the initial period of cell expansion, A_{lumen} shrunk by 30–42% (see Fig. S4 in Supplementary data). During the longer per iod of evaporation, A_{lumen} recovered its original size much faster than A_{lumen}. The values of A_{wall} increased by 53–62% during the initial period of expansion and then completely reverted to their original values during water evaporation over the course of 2 h.

The observed expansion of the ML agrees with the similar observation after displacing EMIMAC with water. Water swells the ML and allows penetration into the cell wall from both sides, whereas EMIMAC has little effect on the ML and penetrates into the cell wall from the lumen. The ability of EMIMAC to reversibly swell the cell wall could be used to introduce materials/chemicals into the cell wall. Their presence can be exploited to report on

changes in cell wall structure and chemical composition, for exam ple nanoparticles for surface-enhanced Raman spectroscopy (Lucas et al., 2010).

3.2. Raman microspectroscopy studies

A Raman spectrum recorded from untreated poplar shows bands that can be assigned to cellulosic, hemicellulosic, and lignin components (see Fig. S5 in Supplementary data). The spectrum recorded from poplar swollen in water contains the same bands but with differences in their relative heights. In particular, the intensity ratio of the 1460 cm^{-1} (cellulose) and the 1604 cm^{-1} (lignin) bands is lower in the water swollen poplar spectrum compared to the dry poplar. This can be interpreted as a decrease in the relative density of the cellulose-rich S2 sub-layer compared to the lignin-rich and more hydrophobic ML as the sample is swollen with water. Since the crystalline cellulose fibers are relatively resistant to water penetration, this swelling must be due to water penetration in between the fibers, pushing the fibers apart, and into less well ordered cellulose. Another major difference between the hydrated and dehydrated samples is a broadening of the bands in the 1274–1454 cm^{-1} range. Deuteration studies previously showed that the hydrogen atoms involved in the vibrational signatures of these bands are labile and subject to hydrogen bonding (Wiley and Atalla, 1987).

The spectrum recorded from neat EMIMAC agrees with those previously reported (Dhumal et al., 2009). When poplar is swollen in EMIMAC, the spectrum is dominated by signatures from EMIMAC, but bands from the underlying lignocellulosic material can still be recorded. Importantly, the spectrum recorded from poplar swollen in EMIMAC and then washed with water exhibits no evidence of any residual EMIMAC and is similar to the spectrum recorded from poplar swollen in water. Indeed, close examination of strong EMIMAC bands, in an otherwise clear region of the poplar spectrum, such as at 600 cm^{-1} or at 960 cm^{-1}, shows no evidence of EMIMAC remaining within the sampling region.

These results indicate that the overall composition of the cell wall is the same after swelling in either water or EMIMAC. There still may be a loss of material during EMIMAC treatment, but if so, it would have occurred equally amongst the cellulose, hemicel-luloses and lignin components. A recent study by Lee et al. (2009) showed no significant change in the relative abundance of the hemicellulose and lignin content in EMIMAC pretreated wood flour until the processing temperature increases above about 90 °C. Furthermore, water would appear to preferentially swell the cellulosic component, dispersing the water impervious crystalline cellulose fibers.

3.3. Scanning microprobe X-ray diffraction studies

The diffraction pattern recorded from the untreated sample is characteristic of cellulose I (Foston et al., 2009; Leppänen et al., 2009; Nishiyama et al., 2002, 2003), but contains two superimposed equators with a relative orientation of approximately 25° (see Fig. S6 in Supplementary data). One possible explanation is that diffraction occurs from both the front and back walls of a cell as the incident X-ray beam passes through the sample. Cellulose microfibrils in the thick S2 layer of poplar cells are known to have a winding angle, referred to as the microfibril angle (MFA), which has been proposed to be related to wood strength. The observed relative orientation of the equators would correspond to a value for the MFA of 12.5° which is in about the middle of the wide range observed for different clones and ring positions in poplar trees (Fang et al., 2006). The measured radial width of the equatorial reflections were used to calculate a Scherrer dimension of 5 nm, as described in previous studies (e.g. Leppänen et al., 2009), but with the Scherrer constant, K, set at a value of 1.0, as discussed by Nishiyama et al. (2010). This value can be related to the approximate width of the microfibrils of cellulose I.

Immediately after application of EMIMAC, the diffraction is dominated by a diffuse ring from the IL. Diffraction from the microfibrils of cellulose I becomes weaker in intensity until it cannot be detected. When water is applied, the diffraction from EMIMAC disappears and the diffraction from cellulose I reappears gradually, notably the two superimposed equators. The disappearance of diffraction from microfibrils of cellulose I on application of EMIMAC and then its reappearance on expulsion of EMIMAC is surprising. This is in sharp contrast to studies of IL pretreatments of biomass at higher temperatures in which the cell wall is observed to swell outwards by a factor of as much as 8 before completely disintegrating. Cellulose is then precipitated in an amorphous form or as the cellulose II phase (Li et al., 2010; Singh et al., 2009), both of which are more easily hydrolyzed by enzymes.

Autofluorescence studies showed that the cell wall swells in towards L only by a factor of two (Fig. 1). If the microfibrils of cellulose I persist during EMIMAC treatment then their density and therefore the diffraction intensity would be expected to decrease only by a factor of two. On the other hand, if the microfibrils of cellulose I are completely solubilized then the cellulose is expected to regenerate in the cellulose II phase with no preferential orientation of the crystal domains. One possible explanation is that because the ML retains its structure during treatment with EMIMAC the cellulose chains released from microfibrils of cellulose I remain constrained in the same parallel orientation within the cell wall as a sol. On expulsion of EMIMAC, the chains do not have sufficient freedom to migrate into the antiparallel arrangement required for crystallization as cellulose II (Langan et al., 1999, 2001) and therefore they recrystallize as cellulose I. Another possible explanation is that most but not all of the microfibrils of cellulose are solubilized. Those few microfibrils that persist then act as sites of nucleaction for cellulose I on expulsion of EMIMAC.

In order to investigate the detailed action of EMIMAC on cellulose further, this experiment was repeated with a ramie fiber. Ramie fibers have a much higher cellulose content (~85%) and lower lignin content (~1%) than the poplar samples in this study and might therefore be expected to be less effected by the lignin structure (Norman, 1936). The initial diffraction pattern recorded from the untreated ramie fiber is characteristic of cellulose I (see Fig. S7 in Supplementary data). The measured Scherrer dimension is 10 nm and the diffraction is clearly more crystalline than that from poplar. The microfibrils do not show any winding (MFA ~0°), but rather are highly oriented in the direction of the ramie fiber. When EMIMAC was applied, the diffraction from cellulose I gradually becomes weaker in intensity over a period of more than an hour, with its relative intensity dropping by a factor of 10 (see Fig. S8 in Supplementary data), until it became almost undetectable. The implication of this result is that the amount of cellulose I decreases by a factor of 10 during EMIMAC treatment. There is a broadening of the profile of the (2 0 0) reflection and also a slight reduction in its peak position in the radial reciprocal space, but little change in the (1 – 1 0) and (1 1 0) profiles or positions (see Fig. S9 in Supplementary data). The (2 0 0) reflection corresponds to the hydrophobic stacking direction of the sheets of hydrogen bonding chains in cellulose I (Nishiyama et al., 2002, 2003). On expulsion of EMIMAC, diffraction corresponding to cellulose I reappeared and its relative intensity recovered its original value. At this point, more EMIMAC was added and the diffraction from microfibrils of cellulose I gradually weakened again.

Extrapolating the observation on ramie fiber to poplar, it would appear that most (~90% in ramie) but not all of the microfibrils of cellulose in S2 are solubilized. Those few microfibrils that persist (~10% in ramie) then act as sites of nucleation for cellulose I on expulsion of EMIMAC. As the microfibrils are exposed to EMIMAC, there is a small decrease in the width of the microfibrils in the sheet stacking direction and a swelling in the

distance between the sheets. This may indicate that the EMIMAC interacts preferentially with microfibrils at the (2 0 0) surfaces.

The observations of recrystallization of cellulose in the cellulose I phase after EMIMAC treatment of poplar and ramie at room temperature are in contrast to reported transitions from cellulose I to II in pulp with a degree of polymerization (DP) of ~570, dissolved in the ionic liquid 1-allyl-3-methylimidazolium chloride, and regen erated into films after IL displacement with water (Zhang et al., 2005). By comparison, ramie is reported to have a DP of between 1800 and 3400 (Brühlmann et al., 2000; Zhou et al., 2004) and poplar a DP of ~2000 (Sierra-Alvarez and Tjeerdsma, 2007). It may be that when poplar is treated with EMIMAC at room temperature the high DP of the cellulose chains prevents chain migration between microfibrils, which is required to achieve an antiparallel chain arrangement required for crystallization as cellulose II (Langan et al., 1999, 2001). Both the disruption of the cell wall and also the conversion of cellulose from cellulose I into another form will be important factors in the effectiveness of these high temperature pretreatments for improving the efficiency of saccharification. Room temperature treatment with EMIMAC achieves neither.

4. Conclusions

Complementary experimental techniques provided new insights into the IL interaction with lignocellulosic biomass at room temperature. When poplar is treated with EMIMAC at room temperature, the cell walls swell by about a factor of two towards the empty lumen. During swelling, most cellulose microfibrils are solubilized but chain migration is restricted and a few microfibrils persist as cellulose I. Upon EMIMAC expulsion, the cellulose recrystallizes as cellulose I microfibrils. Raman spectra showed little change in the cell wall chemical composition after treatment. The action of EMIMAC appears to be a reversible swelling accompanied by a reversible decrystallization of cell wall.

Acknowledgments

The authors thank BIOCAT at the Advanced Photon Source for the use of facilities. Raul Barrea and Joseph Orgel are acknowledged for help with data collection. PL was supported in part by the Office of Biological and Environmental Research of the Department of Energy. PL, ML, KDR and GW were supported in part by a Laboratory Directed Research and Development grant from Los Alamos National Laboratory (20080001DR). CS and IS were partially supported by the Ohio Third Frontier Advanced Energy Program 2009 grant #09-053 with SuGanit Systems.

Appendix A. Supplementary data

Supplementary data associated with this article can be found, in the online version, at doi: 10.1016/j.biortech.2010.12.087.

References

Alvira P, Tomás-Pejó E, Ballesteros M, Negro MJ. Pretreatment technologies for an efficient bioethanol production process based on enzymatic hydrolysis: a review. Bioresour Technol. 2010; 101:4851–4861. [PubMed: 20042329]

Brühlmann F, Leupin M, Erismann KH, Fiechter A. Enzymatic degumming of ramie bast fibers. J Biotechnol. 2000; 76:43–50. [PubMed: 10784295]

Chen Y, Stipanovic AJ, Winter WT, Wilson DB, Kim YJ. Effect of digestion by pure cellulases on crystallinity and average chain length for bacterial and microcrystalline celluloses. Cellulose. 2007; 14:283–293.

Côté WA Jr, Day AC, Timell TE. A contribution to the ultrastructure of tension wood fibers. Wood Sci Technol. 1969; 3:257–271.

Dadi AP, Varanasi S, Schall CA. Enhancement of cellulose saccharification kinetics using an ionic liquid pretreatment step. Biotechnol Bioeng. 2006; 95:904–910. [PubMed: 16917949]

Dadi AP, Schall CA, Varanasi S. Mitigation of cellulose recalcitrance to enzymatic hydrolysis by ionic liquid pretreatment. Appl Biochem Biotechnol. 2007:137–140. 407–422. [PubMed: 18421594]

Dhumal NR, Kim HJ, Kiefer J. Molecular interactions in 1-ethyl-3-methylimidazolium acetate ion pair: a density functional study. J Phys Chem A. 2009; 113:10397–10404. [PubMed: 19711961]

Fang S, Yang W, Tian Y. Clonal and within-tree variation in microfibril angle in poplar clones. New Forests. 2006; 31:373–383.

Fort DA, Remsing RC, Swatloski RP, Moyna P, Moyna G, Rogers RD. Can ionic liquids dissolve wood? Processing and analysis of lignocellulosic materials with 1-*n*-butyl-3-methylimidazolium chloride. Green Chem. 2007; 9:63–69.

Foston M, Hubbell CA, Davis M, Ragauskas AJ. Variations in cellulosic ultrastructure of poplar. Bioenerg Res. 2009; 2:193–197.

Gierlinger N, Schwanninger M. Chemical imaging of poplar wood cell walls by confocal Raman microscopy. Plant Physiol. 2006; 140:1246–1254. [PubMed: 16489138]

Igarashi K, Wada M, Samejima M. Activation of crystalline cellulose to cellulose III_I results in efficient hydrolysis by cellobiohydrolase. FEBS J. 2007; 274:1785–1792. [PubMed: 17319934]

Kosan B, Michels C, Meister F. Dissolution and forming of cellulose with ionic liquids. Cellulose. 2008; 15:59–66.

Langan P, Nishiyama Y, Chanzy H. A revised structure and hydrogen-bonding system in cellulose II from a neutron fiber diffraction analysis. J Am Chem Soc. 1999; 121:9940–9946.

Langan P, Nishiyama Y, Chanzy H. X-ray structure of mercerized cellulose II at 1 Å resolution. Biomacromolecules. 2001; 2:410–416. [PubMed: 11749200]

Lee SH, Doherty VT, Linhardt RJ, Dordick JS. Ionic liquid-mediated selective extraction of lignin from wood leading to enhanced enzymatic cellulose hydrolysis. Biotechnol Bioeng. 2009; 102:1368–1376. [PubMed: 19090482]

Leppänen K, Andersson S, Torkkeli M, Knaapila M, Kotelnikova N, Serimaa R. Structure of cellulose and microcrystalline cellulose from various wood species, cotton and flax studied by X-ray scattering. Cellulose. 2009; 16:999–1015.

Li C, Kneirim B, Manisseri C, Arora R, Scheller HV, Auer M, Vogel KP, Simmons BA, Singh S. Comparison of dilute acid and ionic liquid pretreatment of switchgrass: biomass recalcitrance, delignification and enzymatic saccharification. Bioresour Technol. 2010; 101:4900–4906. [PubMed: 19945861]

Lucas M, Macdonald BA, Wagner GL, Joyce SA, Rector KD. Ionic liquid pretreatment of poplar wood at room temperature: swelling and incorporation of nanoparticles. ACS Appl Mater Interfaces. 2010; 2:2198–2205. [PubMed: 20735091]

Nishiyama Y, Langan P, Chanzy H. Crystal structure and hydrogen-bonding system in cellulose I_β from synchrotron X-ray and neutron fiber diffraction. J Am Chem Soc. 2002; 124:9074–9082. [PubMed: 12149011]

Nishiyama Y, Sugiyama J, Chanzy H, Langan P. Crystal structure and hydrogen bonding system in cellulose I_α from synchrotron X-ray and neutron fiber diffraction. J Am Chem Soc. 2003; 125:14300–14306. [PubMed: 14624578]

Nishiyama Y, Wada M, Hanson BL, Langan P. Time-resolved X-ray diffraction microprobe studies of the conversion of cellulose I to ethylenediamine-cellulose I. Cellulose. 2010; 17:714–735.

Norman AG. The composition of some vegetable fibres with particular reference to jute. Biochem J. 1936; 30:831–838. [PubMed: 16746095]

Romero A, Santos A, Tojo J, Rodríguez A. Toxicity and biodegradability of imidazolium ionic liquids. J Hazard Mater. 2008; 151:268–273. [PubMed: 18063302]

Sannigrahi P, Ragauskas AJ, Tuskan GA. Poplar as a feedstock for biofuels: a review of compositional characteristics. Biofuels, Bioprod Biorefin. 2010; 4:209–226.

Samayam IP, Schall CA. Saccharification of ionic liquid pretreated biomass with commercial enzyme mixtures. Bioresour Technol. 2010; 101:3561–3566. [PubMed: 20096568]

Sierra-Alvarez R, Tjeerdsma BF. Organosolv pulping of poplar wood from short-rotation intensive culture plantations. Wood Fiber Sci. 2007; 27:395–401.

Singh S, Simmons BA, Vogel KP. Visualization of biomass solubilization and cellulose regeneration during ionic liquid pretreatment of switchgrass. Biotechnol Bioeng. 2009; 104:68–75. [PubMed: 19489027]

Sun N, Rahman M, Qin Y, Maxim ML, Rodríguez H, Rogers RD. Complete dissolution and partial delignification of wood in the ionic liquid 1-ethyl-3-methylimidazolium acetate. Green Chem. 2009; 11:646–655.

Wada M, Chanzy H, Nishiyama Y, Langan P. Cellulose III_I crystal structure and hydrogen bonding by synchrotron X-ray and neutron fiber diffraction. Macromolecules. 2004; 37:8548–8555.

Wiley JH, Atalla RH. Band assignments in the Raman spectra of celluloses. Carbohydr Res. 1987; 160:113–129.

Yang B, Wyman CE. Pretreatment: the key to unlocking low-cost cellulosic ethanol. Biofuels, Bioprod Biorefin. 2008; 2:26–40.

Zhang H, Wu J, Zhang J, He J. 1-Allyl-3-methylimidazolium chloride room temperature ionic liquid: a new and powerful nonderivatizing solvent for cellulose. Macromolecules. 2005; 38:8272–8277.

Zhou LM, Yeung KW, Yuen CWM, Zhou X. Characterization of ramie yarn treated with sodium hydroxide and crosslinked by 1, 2, 3, 4-butanetetracarboxylic acid. J Appl Polym Sci. 2004; 91:1857–1864.

Zhu S, Wu Y, Chen Q, Yu Z, Wang C, Jin S, Ding Y, Wu G. Dissolution of cellulose with ionic liquids and its application: a mini-review. Green Chem. 2006; 8:325–327.

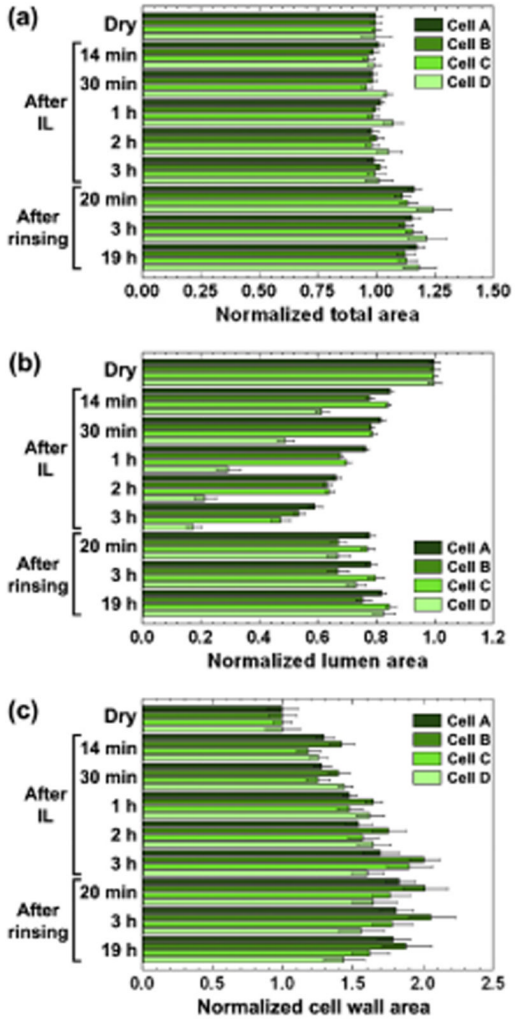

Fig. 1.

(a) Total cell area, (b) lumen area, and (c) their difference as a function of time for four cells A–D during the ionic liquid (IL) pretreatment and after rinsing with de-ionized water.